3496 *Chem. Mater.* **2010,** *22,* 3496–3501
DOI:10.1021/cm1006229

CHEMISTRY OF MATERIALS
Article

Effect of Solvent Treatment on Solution-Processed Colloidal PbSe Nanocrystal Infrared Photodetectors

Galileo Sarasqueta,[†] Kaushik Roy Choudhury,[†] and Franky So*

Department of Materials Science and Engineering, University of Florida, Gainesville, Florida 32611-6400.
[†]These authors contributed equally to this work.

Received March 1, 2010. Revised Manuscript Received April 23, 2010

PbSe colloidal nanocrystals were used to fabricate infrared photodetectors. Low dark currents were obtained by using chemical treatments to improve the nanocrystal film quality and passivate traps in the nanocrystals. The effects of different nanocrystal capping groups, including oleic acid, octylamine, ethanedithiol, and benzenedithiol, on the nanocrystal film quality and the photodiode characteristics were studied. The spectral responsivities and quantum efficiencies of the photodetectors were also measured. We found that the physical quality of the films was very sensitive to the capping groups used for the nanocrystals as well as the specific exchange reactions. Specifically, the dithiol capping groups were found to enhance the rectification of the photodetectors and significantly reduce the dark current in the devices by effectively passivating the surface traps.

1. Introduction

The ability to detect infrared light with high sensitivity is of paramount importance for diagnostic and therapeutic medical, remote sensing, and night-vision applications. Solution-processed light-sensing semiconductor optoelectronic devices offer the possibility of low-cost manufacturing and compatibility with flexible electronics. While significant progress has been made in solution-processed organic-based photodetectors, the bandgap of these materials limits their use to wavelengths shorter than 1 μm.[1,2] Colloidal inorganic nanocrystals based on III−V and IV−VI semiconductors can overcome this limitation by extending the detector sensitivities to longer wavelengths.[3,4] These nanocrystals can be synthesized using wet-chemical techniques and can be processed from solutions at low temperatures. They offer the advantage of bandgap tunability over a wide wavelength range because of the quantum size effect, allowing for spectral selectivity. Significant progress has been made over the past few years in realizing infrared photodetectors using solution-processed colloidal nanocrystals. Photodetectors have been demonstrated using neat nanocrystal thin films as well as thin films of hybrid bulk−heterojunction blend composites with polymers[5,6] as the photoactive layers.[4,7,8] The polymer-based composite devices often have a limited absorption range, low carrier mobility, and poor device stability compared with crystalline inorganic semiconductor photodetectors. On the other hand, photoconductive devices based on nanocrystal thin films with high efficiencies have been reported.[7,8] However, these devices suffer from high dark currents. An important performance parameter for detectors is their signal-to-noise (S/N) ratio. To obtain a device with a high S/N ratio, the detector responsivity needs to be high while the dark current needs to be low. In this study, we explore the fabrication of infrared photodetectors from colloidal PbSe nanocrystals in achieving low dark currents and a good photoresponse.

One of the challenges that needs to be overcome in employing colloidal nanocrystals in optoelectronic devices is the poor charge transport properties of neat nanocrystal films.[9] Because of the characteristic hopping mechanism[13] responsible for the transport of charge between nanocrystals, the electronic nature of the capping ligands plays an important role in determining the transport properties. The spatial separation between neighboring nanocrystals determines the width of the energy barrier through which carriers need to tunnel to reach an adjacent nanocrystal. This affects the overall mobility as well as the conductivity of the nanocrystal films. Semiconductor nanocrystals are typically synthesized with long aliphatic ligands to enable easy processing and prevent aggregation in solution. However, since the

*To whom correspondence should be addressed. E-mail: fso@mse.ufl.edu. Telephone: (352) 846-3790.

(1) Yao, Y.; Liang, Y.; Shrotriya, V.; Xiao, S.; Yu, L.; Yang, Y. *Adv. Mater.* **2007**, *19*, 3979–3983.
(2) Hwang, I.-W.; Soci, C.; Moses, D.; Zhu, Z.; Waller, D.; Gaudiana, R.; Brabec, C. J.; Heeger, A. J. *Adv. Mater.* **2007**, *19*, 2307–2312.
(3) Sargent, E. H. *Adv. Mater.* **2008**, *20*, 3958–3964.
(4) Böberl, M.; Kovalenko, M. V.; Gamerith, S.; List, E. J. W.; Heiss, W. *Adv. Mater.* **2007**, *19*, 3574–3578.
(5) Choudhury, K. R.; Sahoo, Y.; Ohulchanskyy, T. Y.; Prasad, P. N. *Appl. Phys. Lett.* **2005**, *87*, 073110.
(6) McDonald, S. A.; Konstantatos, G.; Zhang, S. G.; Cyr, P. W.; Klem, E. J. D.; Levina, L.; Sargent, E. H. *Nat. Mater.* **2005**, *4*, 138.
(7) Konstantatos, G.; Howard, I.; Fischer, A.; Hoogland, S.; Clifford, J.; Klem, E.; Levina, L.; Sargent, E. H. *Nature* **2006**, *442*, 180.
(8) Konstantatos, G.; Clifford, J.; Levina, L.; Sargent, E. H. *Nat. Photonics* **2007**, *1*, 531.
(9) Jarosz, M. B.; Porter, V. J.; Fisher, B. R.; Kastner, M. A.; Bawendi, M. G. *Phys. Rev. B* **2004**, *70*, 195327.

 Published on Web 05/11/2010

spacing between individual nanocrystals is determined by the length of the organic ligands, films made from such nanocrystals are highly insulating. Exchange of the long ligands with shorter and preferably more conducting ones is required to ensure good carrier transport in the nanocrystal films. At the same time, two other considerations need to be kept in mind while such an exchange of surface ligands is performed: passivation of the nanocrystal surfaces during the ligand exchange reaction to maintain their chemical stability and loss of free volume leading to the development of cracks in the nanocrystal films. Recently, the use of thiol-terminated short-chain ligands and cross-linkers to improve the responsivity of nanocrystal photodetectors has been reported.[8,10−12] In this paper, we study the effect of different organic surface capping ligands, including oleic acid, octylamine, ethanedithiol (EDT), and benzenedithiol (BDT), on film formation. In addition, we have also studied the electrical properties of the treated films and the device characteristics of the resulting infrared photodiodes.

2. Experimental Section

We investigated the effect of capping moieties on the device characteristics of PbSe nanocrystal infrared photodetectors. The colloidally synthesized PbSe nanocrystals used in this study are passivated with long-chain aliphatic oleic acid capping groups. Since close packing among nanocrystals is required for efficient charge carrier transport, we replaced the insulating oleate ligands with shorter ligands such as octylamine, ethanedithiol, and benzenedithiol. To obtain smooth, defect-free, good-quality films from a solution of dispersed nanocrystals, one also needs to consider the loss of free volume during the ligand exchanging process. We observed cracks and pinholes formed due to the strain developed in the films as a result of the ligand exchange reaction. To improve the film quality, during the ligand exchange reaction, we employed a two-step ligand exchange process with a solution-phase exchange followed by a cross-linking process in the solid state.

2.1. Synthesis of PbSe Nanocrystals. PbSe nanocrystals were synthesized using modified versions of established organometallic synthetic routes[14] via addition of diphenylphosphine (DPP) as a catalyst. In a typical reaction, lead oxide (2 mmol) was dissolved in a mixture of octadecene and oleic acid (6 mmol) under uniform heating, vigorous stirring, and a constant flow of argon. Once the temperature reached 140 °C, 6 mmol of a 1 M solution of selenium in trioctylphospine and 56 μL of DPP were rapidly injected into the mixture to initiate nucleation of nanocrystals. The size of the nanocrystals is determined by the reaction time. To terminate the reaction, cold toluene was injected into the reaction mixture. The resulting nanocrystals were subsequently washed via precipitation with acetone and redispersion in toluene, and the process was repeated three times to eliminate the excess unreacted precursors and reaction byproducts.

2.2. Exchange of Nanocrystal Passivating Ligands in Solution. In the ligand exchange reaction, the bulky (~2 nm in length) oleate ligands were exchanged with shorter-chain (~1 nm) octylamine. This postsynthetic solution-phase exchange was performed in a nitrogen glovebox. To replace the ligands with octylamine, the nanocrystals were precipitated using acetone and then redispersed in 10 mL of octylamine. The ligand exchange solution was left stirring at room temperature for 48 h to allow the maximum exchange of ligands. Subsequently, the nanocrystals were precipitated with acetone and finally redispersed in chloroform, yielding a typical concentration of 60 mg/mL. The exchange of oleate passivating groups with octylamine resulted in a clear dispersion with no agglomeration of nanocrystals.

2.3. Device Fabrication and Solid-State Treatment. To deposit the nanocrystal films for device fabrication, PbSe nanocrystals with either oleic acid or octylamine capping groups were spin-coated on UV- and ozone-treated ITO-coated glass substrates inside a nitrogen glovebox. Subsequently, the samples were immersed in a 0.1 M solution of EDT or BDT in acetonitrile for 30 s, and then the films were rinsed with acetonitrile or chloroform to remove any loose agglomerates and residue. The samples were subsequently dried inside the glovebox. This solid-state treatment rendered the nanocrystal layer insoluble in solvents used for further device processing. To reduce the frequency of pinholes and cracks, multiple nanocrystal layers were spin-coated on top of the substrates. The resulting thin films had a thickness of ca. 200 nm, as measured with a surface profilometer. Finally, a 100 nm thick Al cathode was thermally deposited under vacuum at a pressure ~10^{-6} Torr through a shadow mask with an active area of 4 mm^2. The final device has an ITO−PbSe−Al structure. To study the carrier transport properties, single-carrier devices were also fabricated. To fabricate hole-only devices, the Al electrode was replaced with a Au cathode (50 nm). To fabricate electron-only devices, the ITO substrates were cleaned without UV−ozone treatment to suppress hole injection.

Achieving defect-free, spatially uniform, smooth films is a key requirement to realizing good-quality devices. Because of the difference in the length of the ligands and their chemical nature, it is expected that different ligands lead to different film morphologies. To confirm the exchange of organic ligands on the surface of nanocrystals, Fourier transform infrared spectroscopy (FTIR) was performed. The effect of different surface passivating ligands on the optical properties and the film quality was investigated via spectrophotometry, scanning electron microscopy (SEM), atomic force spectroscopy (AFM), and transmission electron spectroscopy (TEM).

2.4. Device Characterization. The current−voltage ($I-V$) characteristics of the devices were measured with a Keithley 4200 semiconductor parameter analyzer. The devices were irradiated with monochromatic light from a Newport monochromator using an Oriel solar simulator as a source. The illumination intensities were measured using two calibrated Newport 918D photodiodes, one for the visible and the other for the infrared part of the spectrum. To obtain the spectral response of the photodetectors, light from the monochromator was chopped at 400 Hz to modulate the optical signal. The photocurrent response as a function of bias voltage was measured using a Stanford Research System SR810 DSP lock-in amplifier. To gain further insight into the mechanism of charge transport in the devices, the dark $I-V$ characteristics were measured as a function of temperature using a cryostat interfaced with a LakeShore 321 Autotuning temperature controller. The operating temperature was varied from 130 to 310 K.

(10) Barkhouse, D. A. R.; Pattantyus-Abraham, A. G.; Levina, L.; Sargent, E. H. *ACS Nano* **2008**, *2*, 2356.
(11) Koleilat, G.; Levina, L.; Shukla, H.; Myrskog, S. H.; Hinds, S.; Pattantyus-Abraham, A. G.; Sargent, E. H. *ACS Nano* **2008**, *2*, 833.
(12) Williams, K. J.; Tisdale, W. A.; Leschkies, K. S.; Haugstad, G.; Norris, D. J.; Aydil, E. S.; Zhu, X.-Y. *ACS Nano* **2009**, *3*, 1532.
(13) Yu, D.; Wang, C.; Wehrenberg, B. L.; Guyot-Sionnest, P. *Phys. Rev. Lett.* **2004**, *92*, 216802-1.
(14) Steckel, J. S.; Yen, B. K. H.; Oertel, D. C.; Bawendi, M. G. *J. Am. Chem. Soc.* **2006**, *128*, 13032.

3. Results and Discussion

Figure 1 shows the structure of the different capping ligands used in this work and the TEM images of the nanocrystals capped with each of them. As is evident from the TEM images, replacing the oleate ligands with octylamine clearly reduces the spacing between adjacent nanocrystals. In the case of the dithiol capping group in Figure 1c (BDT), the interparticle spacing is further reduced because the thiol end groups interpenetrate each other and cross-link the adjacent nanocrystals. This cross-linking reaction results in nanocrystal films that are insoluble in common organic solvents. In addition, the loss of free volume during the ligand exchange process leads to stress buildup and the formation of pinholes and cracks. These effects are apparent in panels A−C of Figure 2 showing AFM images of nanocrystal films with different capping ligands and chemical treatments. To avoid this detrimental effect on film morphology, we add an intermediate step to exchange the oleate capping groups with shorter ones (octylamine) prior to the dithiol treatments. When this intermediate solution-phase exchange reaction was performed prior to the treatments with EDT or BDT, the number of pinholes and the level of film cracking were greatly reduced as shown in Figure 2D−F. It is also worth noting the difference in film quality between the EDT-treated films and the BDT-treated films. Independent of whether the films were deposited from a batch of oleic acid-capped nanocrystals or octylamine-capped nanocrystals, it is clear from panels B and C of Figure 2 that the EDT treatment affects film morphology more strongly than the BDT treatment. Two factors should be noted. (1) The short dithiol molecules replace the longer capping ligands. (2) The dithiol molecules also draw the nanocrystals closer together by linking them with their thiol end groups. Since EDT molecules are shorter and less bulky than BDT, the free volume loss in the EDT-treated films is greater, resulting in the greater residual stress compared with the BDT-treated films. As a result, we see that in identical nanocrystal films, in panels B and C of Figure 2, cracking is more prevalent in the EDT-treated films. To confirm the chemical changes on the surface of the nanocrystals and in the films brought about by the ligand exchange reaction, we investigated films of PbSe nanocrystals by FTIR in the reflectance mode. Figure 3a compares the FTIR spectrum of a film of PbSe nanocrystals capped with oleic acid with that of another nanocrystal film capped with octylamine ligands. As expected, there is a decrease in the intensity of the C−H peaks after the exchange of oleic acid ligands with shorter-chain octylamine because of the lower content of carbon atoms in the latter. In addition, the N−H peak from the amine group appears in the film containing nanocrystals capped with octylamine. Figure 3b confirms the second stage of ligand exchange. It compares the film of octylamine-capped nanocrystals with a nanocrystal film treated with BDT. The data from the latter show a further reduction of the magnitude of the C−H peaks along with the appearance of sharp C=C peaks originating from the benzene

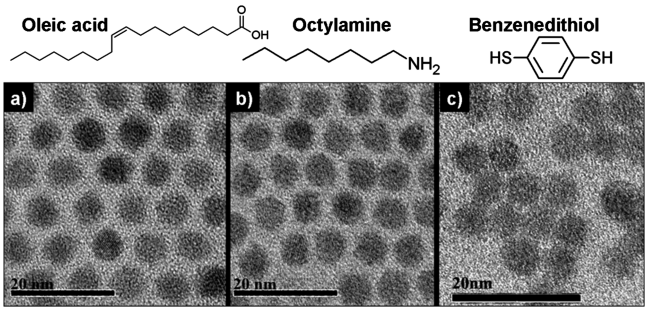

Figure 1. Surface passivating ligands used in this work and TEM images of nanocrystals capped with (a) oleic acid and after exchange of capping ligands with (b) octylamine and (c) benzenedithiol.

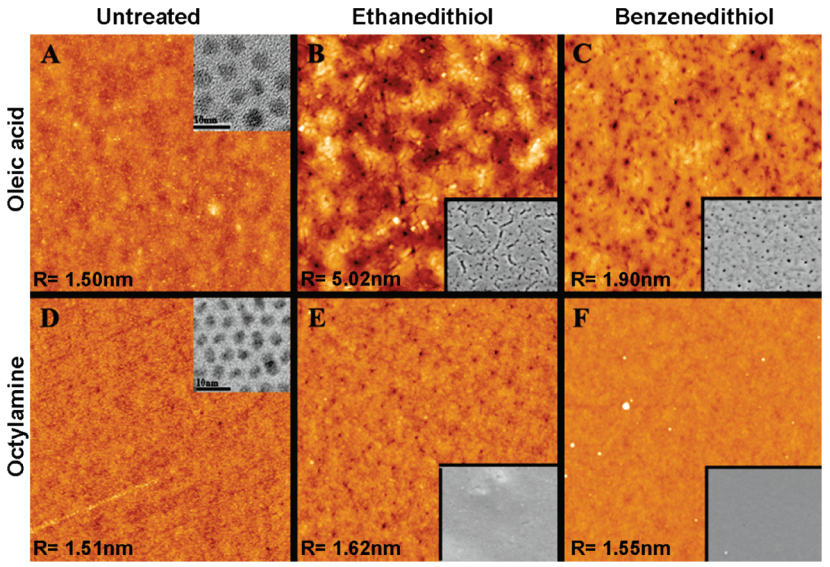

Figure 2. AFM images of films of nanocrystals with different capping ligands and treatments. Images A−C are films of nanocrystals capped with oleic acid, and images D−F are films of nanocrystals capped with octylamine. No treatment in panels A and D. Insets of panels A and D show TEM images of nanocrystals. Films in panels B and E were treated with EDT and films in panels C and F treated with BDT. All AFM images are 5 μm × 5 μm and show their respective roughness at the bottom. Insets of panels B, C, E, and F are SEM images and share the same scale with the AFM images. All films are of the same thickness (150 nm).

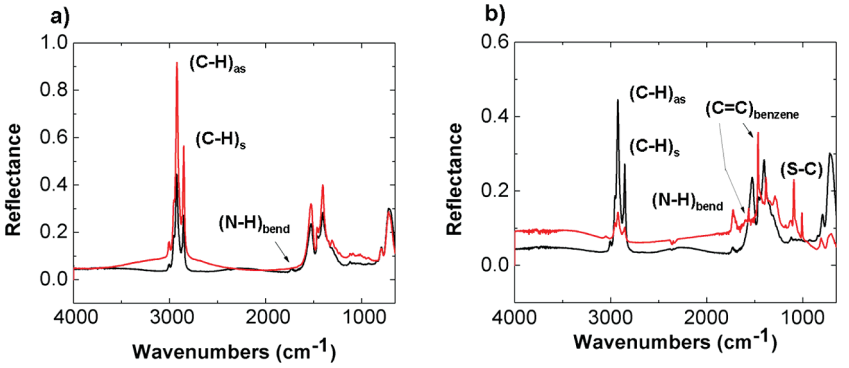

Figure 3. FTIR data showing the comparison between (a) oleic acid-capped nanocrystals (red) and octylamine-capped nanocrystals (black) and (b) octylamine-capped nanocrystals (black) and BDT-treated nanocrystals (red). $(C-H)_s$ and $(C-H)_{as}$ denote symmetrical and asymmetrical peaks, respectively.

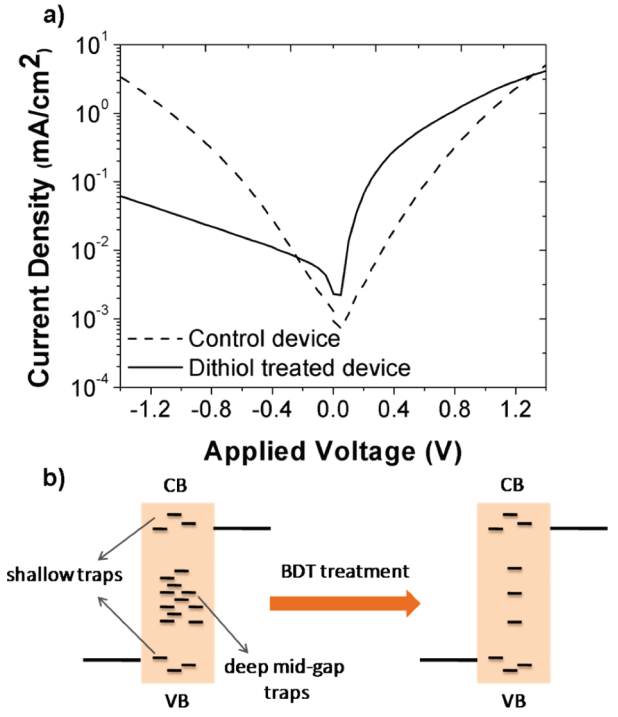

Figure 4. (a) Dark $I-V$ characteristics of PbSe nanocrystal photodetectors capped with different ligands. The plot shows data for an untreated device (octylamine-capped) compared to a device treated with BDT after film formation. (b) Schematic showing the passivation of traps in the nanocrystal thin film by BDT treatment.

ring of the dithiol capping ligand. The presence of a C−O peak at 1520 cm^{-1} in the octylamine-capped nanocrystal film shows some residual oleic acid. This peak is completely suppressed in the spectrum of the BDT-treated film, confirming the efficient ligand exchange.

Replacing the long insulating ligands with interpenetrating and cross-linking short ones not only affects the thin-film quality but also significantly affects the charge transport properties. Figure 4a compares the dark steady-state $I-V$ characteristics of two ITO−PbSe−Al nanocrystal photodetectors with and without the BDT treatment. The plots show the effects of dithiol treatment on the transport characteristics of the nanocrystal films. First, under forward bias, especially at low electric fields, the current density in the device treated with BDT is 2 orders of magnitude higher than that in the untreated device. Second, the untreated device shows a symmetrical $I-V$ curve. The device treated with BDT, on the other hand, exhibits distinct rectification in the $I-V$ characteristics. The enhanced device current under forward bias can be attributed to a decrease in interparticle spacing caused by the short-chain BDT ligand, which leads to enhanced carrier mobility and film conductivity.[15] The absence of rectification in the untreated devices is probably due to a large density of trap states present at the surfaces of the nanocrystals,[9,16] which serve as transport pathways and recombination centers. This situation is shown schematically in Figure 4b. The presence of these deep traps can provide pathways for carrier transport through the midgap states. Because of the presence of these midgap states, the Fermi level is pinned and carriers are injected directly into these gap states under both forward and reverse biases, leading to symmetrical $I-V$ characteristics without any rectification. Here, the BDT treatment serves two functions: it reduces the spacing between adjacent nanocrystals and passivates the surface dangling bonds. As a consequence, carrier transport occurs via electronic states close to the conduction and valence bands of the nanocrystals, resulting in rectification in the $I-V$ characteristics. To further understand how the carrier transport was affected by the BDT treatment in the nanocrystal films,[16,17] we fabricated both electron- and hole-only devices using the PbSe nanocrystals. Estimated from the space charge limited current, the hole and electron mobilities in the BDT-treated devices were estimated to be 2×10^{-4} and 6.5×10^{-4} $cm^2\,V^{-1}\,s^{-1}$, respectively. As expected, compared to untreated PbSe films, the mobilities in BDT-treated films are significantly higher, with a 20-fold increase in hole mobility and a 80-fold increase in electron mobility. The increase in carrier mobility upon treatment of the nanocrystal films with BDT further demonstrates the effect of the thiol-terminated cross-linker in decreasing interparticle spacing and reducing the trap density in the PbSe nanocrystal films.

To gain further insight into the role of the thiol-terminated capping groups in passivating traps in the

(15) Sargent, E. H. *Nat. Photonics* **2009**, *3*, 325.
(16) Ginger, D. S.; Greenham, N. C. *J. Appl. Phys.* **2000**, *87*, 1361.
(17) Li, L.; Meller, G.; Kosina, H. *Solid-State Electron.* **2007**, *51*, 445.

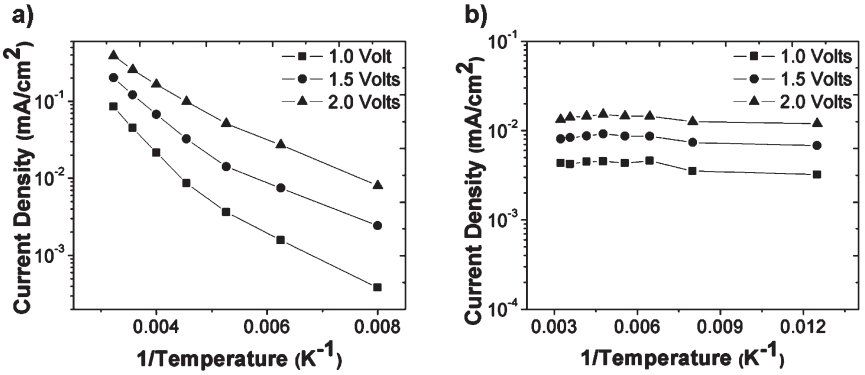

Figure 5. Dark current densities as a function of temperature in nanocrystal photodetector devices after treatment with (a) BDT and (b) octylamine capping groups.

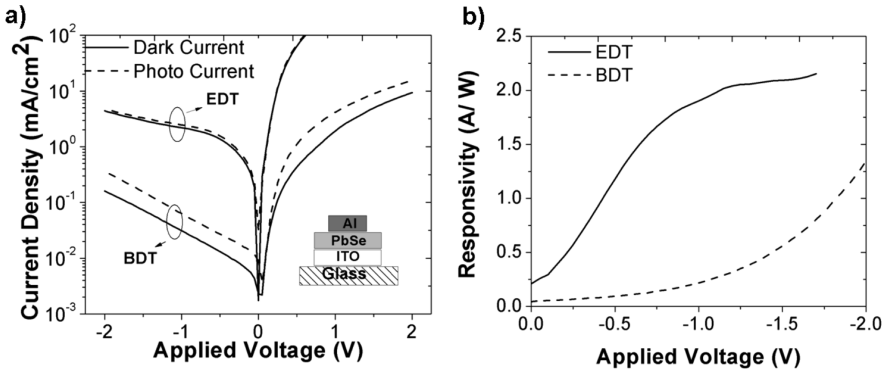

Figure 6. (a) Dark and photo $I-V$ for two nanocrystal photodetector devices treated with EDT or treated with BDT. The devices were illuminated with monochromatic IR light at 830 nm. The inset shows the device architecture. (b) Responsivity plotted as a function of applied reverse bias for the same devices.

nanocrystal thin films, we investigated the temperature dependence of the dark current in the devices. Panels a and b of Figure 5 demonstrate the dark current densities as a function of temperature in the films with and without BDT treatment, respectively. In the devices treated with BDT, the dark current exhibits a temperature dependence with an activation energy of ~25 meV, indicating the transport is a thermally activated process. Similar results were obtained for EDT-treated devices as well. On the other hand, in the device without the dithiol treatment, the current does not show any temperature dependence. The absence of temperature dependence of the device current suggests that the transport is via tunneling through the gap states. These results indicate, as stated earlier, that the dithiol treatments help reduce the density of gap states.

For photodetector applications, achieving low dark currents while maintaining the maximum possible photocurrents is desirable. As discussed in the previous section, photodiode characteristics were only obtained when the PbSe films were treated EDT and BDT. Here, we compared the effect of the two chemical treatments on the photoresponse of the resulting nanocrystal photodetectors. Figure 6a shows the dark currents and photocurrents for photodetectors treated with EDT and BDT. For photocurrent measurements, the devices were illuminated with monochromatic light at 830 nm. The results clearly show that the BDT treatment lowers the dark current in the devices to a greater extent than the EDT treatment. This difference comes from the molecular structure of the linking groups and the packing density of nanocrystals. Because EDT is a shorter linear molecule than BDT, the nanocrystals can be packed closer together, leading to a higher device dark current in the device. The responsivity of the photodetectors can be determined using the following expression:

$$\text{responsivity} = J_{\text{photo}}(\lambda)/P_{\text{d}} \qquad (1)$$

where $J_{\text{photo}}(\lambda)$ is the photocurrent density of the device at a specific illumination wavelength and P_{d} is the incident light power density. Figure 6b shows the responsivities for the two devices as a function of bias voltage. The EDT-treated device exhibits a responsivity larger than 0.67 A/W at low voltages, indicating that there is gain in the photoresponse at reverse bias voltages larger than −0.26 V. Gain in organic photodetectors with high dark currents has been observed and attributed to enhanced charge injection from the electrode due to accumulation of photogenerated carriers trapped at the electrode interface.[18−21] On the other hand, gain was

(18) Matsukura, Y.; Uchiyama, Y.; Yamashita, H.; Nishino, H.; Fujii, T. *Infrared Phys. Technol.* **2009**, *52*, 257.
(19) Gao, J.; Hegmann, F. A. *Appl. Phys. Lett.* **2008**, *93*, 223306.
(20) Hiramoto, M.; Miki, A.; Yoshida, M.; Yokoyama, M. *Appl. Phys. Lett.* **2002**, *81*, 1500.
(21) Hiramoto, M.; Imahigashi, T.; Yokoyama, M. *Appl. Phys. Lett.* **1994**, *64*, 187.

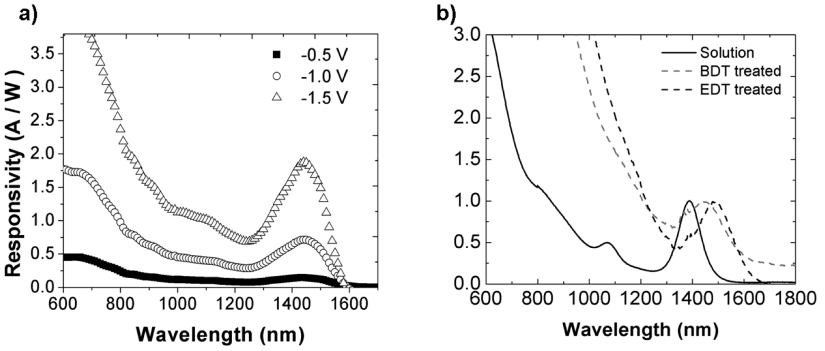

Figure 7. (a) Spectral response as a function of wavelength at different voltages for a different PbSe photodetector device, which was treated with BDT. (b) Absorption spectrum of nanocrystals in solution and in films after they have been treated with BDT or EDT.

not observed in BDT-treated devices at low voltages because of the low dark currents. However, at higher voltages, the dark current increases, resulting in gain at voltages beyond −1.7 V. Since gain in photodetectors is usually associated with traps and high dark currents,[21] these results suggest that the EDT-treated devices have a higher trap density, resulting in gain and higher dark currents compared to those of BDT-treated devices at low voltages.

An important performance parameter in photodetectors is the spectral width over which they are active. PbSe nanocrystals, by virtue of quantum size effects, allow tuning of the absorption edge over a broad range of wavelengths in the infrared. Consequently, the cutoff wavelength of the photodetectors can also be tuned easily. Also, because of the spectral sensitivity of the nanocrystals all the way into visible wavelengths, the detectors display a broad window of activity. Figure 7a shows the spectral response of a photodetector device at different reverse bias voltages. The shape of the responsivity closely follows the absorption spectrum (shown in Figure 7b) of the BDT-treated nanocrystal films. The peak in absorption and responsivity at 1450 nm is attributed to the first excitonic transition in the nanocrystals. These data confirm that the nanocrystals act as IR sensitizers in these devices. Figure 7b also shows the absorption of the nanocrystals in solution. It is interesting to note that there is a shift in the absorption peak of the films to longer wavelengths after they are treated with the dithiol solutions. This shift is expected, since the treatment with EDT or BDT cross-links the nanocrystals and reduces interparticle distances to increase the effective cluster size. These shifts also suggest that in addition to nanocrystal size, the cutoff wavelength of the photodetectors can be controlled via the chemical treatments.

4. Conclusions

In conclusion, we demonstrated in detail the direct effect of surface treatments on the device characteristics of colloidal nanocrystal photodetectors. More specifically, the ability of the capping groups to alter the density of trap states in the PbSe nanocrystals is extremely important for obtaining rectification and reducing dark currents. At the same time, fabrication of defect-free films is of utmost importance in these solution-processed nanocrystal films. This is achieved through an intermediate ligand exchange step in solution prior to the treatment of films in the solid state. Greatly reduced dark current densities were achieved in IR photodetectors employing short-chain BDT capping ligands, maintaining good responsivity in the devices across a broad spectral range.

Acknowledgment. We gratefully acknowledge financial support for the research from DARPA (Contract W31P4Q0910017). We also thank the Major Analytical Instrumentation Center for the support of characterization facilities.